NASA/TM—2015-218743

A Summary of the Space-Time Conservation Element and Solution Element (CESE) Method

Xiao-Yen Wang
Glenn Research Center, Cleveland, Ohio

June 2015

NASA STI Program . . . in Profile

Since its founding, NASA has been dedicated to the advancement of aeronautics and space science. The NASA Scientific and Technical Information (STI) Program plays a key part in helping NASA maintain this important role.

The NASA STI Program operates under the auspices of the Agency Chief Information Officer. It collects, organizes, provides for archiving, and disseminates NASA's STI. The NASA STI Program provides access to the NASA Technical Report Server—Registered (NTRS Reg) and NASA Technical Report Server—Public (NTRS) thus providing one of the largest collections of aeronautical and space science STI in the world. Results are published in both non-NASA channels and by NASA in the NASA STI Report Series, which includes the following report types:

- TECHNICAL PUBLICATION. Reports of completed research or a major significant phase of research that present the results of NASA programs and include extensive data or theoretical analysis. Includes compilations of significant scientific and technical data and information deemed to be of continuing reference value. NASA counter-part of peer-reviewed formal professional papers, but has less stringent limitations on manuscript length and extent of graphic presentations.

- TECHNICAL MEMORANDUM. Scientific and technical findings that are preliminary or of specialized interest, e.g., "quick-release" reports, working papers, and bibliographies that contain minimal annotation. Does not contain extensive analysis.

- CONTRACTOR REPORT. Scientific and technical findings by NASA-sponsored contractors and grantees.

- CONFERENCE PUBLICATION. Collected papers from scientific and technical conferences, symposia, seminars, or other meetings sponsored or co-sponsored by NASA.

- SPECIAL PUBLICATION. Scientific, technical, or historical information from NASA programs, projects, and missions, often concerned with subjects having substantial public interest.

- TECHNICAL TRANSLATION. English-language translations of foreign scientific and technical material pertinent to NASA's mission.

For more information about the NASA STI program, see the following:

- Access the NASA STI program home page at http://www.sti.nasa.gov

- E-mail your question to help@sti.nasa.gov

- Fax your question to the NASA STI Information Desk at 757-864-6500

- Telephone the NASA STI Information Desk at 757-864-9658

- Write to:
  NASA STI Program
  Mail Stop 148
  NASA Langley Research Center
  Hampton, VA 23681-2199

NASA/TM—2015-218743

A Summary of the Space-Time Conservation Element and Solution Element (CESE) Method

Xiao-Yen Wang
Glenn Research Center, Cleveland, Ohio

National Aeronautics and
Space Administration

Glenn Research Center
Cleveland, Ohio 44135

June 2015

Acknowledgments

The author acknowledges valuable input from Drs. Hung Huynh, Philip Jorgenson, Ken Loh, Wai-Ming To, Balaji Venkatachari, Chau-Lyan Chang, and Sin-Chung Chang. The support from Mrs. Mary Jo Davis, Dr. James DeBonis, and Dr. James Heidmann is greatly appreciated. This work was funded by the Transformative Tools and Technologies project under NASA's Fundamental Aeronautics Program.

This report is a formal draft or working paper, intended to solicit comments and ideas from a technical peer group.

This report contains preliminary findings, subject to revision as analysis proceeds.

This work was sponsored by the Fundamental Aeronautics Program at the NASA Glenn Research Center.

Level of Review: This material has been technically reviewed by technical management.

Available from

NASA STI Program
Mail Stop 148
NASA Langley Research Center
Hampton, VA 23681-2199

National Technical Information Service
5285 Port Royal Road
Springfield, VA 22161
703-605-6000

This report is available in electronic form at http://www.sti.nasa.gov/ and http://ntrs.nasa.gov/

A Summary of the Space-Time Conservation Element and Solution Element (CESE) Method

Xiao-Yen Wang
National Aeronautics and Space Administration
Glenn Research Center
Cleveland, Ohio 44135

Summary

The space-time Conservation Element and Solution Element (CESE) method for solving conservation laws is examined for its development motivation and design requirements. The characteristics of the resulting scheme are discussed. The discretization of the Euler equations is presented to show readers how to construct a scheme based on the CESE method. The differences and similarities between the CESE method and other traditional methods are discussed. The strengths and weaknesses of the method are also addressed.

1.0 Introduction

The space-time Conservation Element and Solution Element (CESE) method was introduced by S.-C. Chang (Ref. 1) in 1995 as shown in the Figure 1 timeline. In 1999, the two-dimensional (2D) triangular and three-dimensional (3D) tetrahedral unstructured Euler solvers were published (Refs. 2 and 3), which was followed by the extension to the 2D quadrilateral and 3D hexahedral meshes by Zhang (Ref. 4) in 2002. The Courant number (i.e., Courant-Friedrichs-Lewy (CFL) number) insensitive scheme was presented in 2002 (Ref. 5) and 2003 (Ref. 6) and gave users a better way to minimize the numerical dissipation. In the same year, Huynh published a paper to address the similarities and differences between CESE and other methods (Ref. 7) and gave an insightful view of the CESE method. Local time stepping was introduced in 2005 (Ref. 8) for time-accurate Euler solutions, whereby different timescales are used in the computational domain and the time step at each mesh point can vary during the time-marching to achieve higher CFL numbers at all locations and all the time. This results in better accuracy (less dissipation) and less computational time. The 2D/3D Navier-Stokes solver was published by C.-L. Chang in 2006 (Ref. 9) and 2007 (Ref. 10). In 2010, the high-order (fourth-order) CESE scheme was introduced by S.-C. Chang (Ref. 11) and was extended to the 2D Euler equations in 2013 (Ref. 12) and 2014 (Ref. 13). The strategy for handling meshes with a high aspect ratio (a viscous mesh near a solid wall) is described in Reference 14.

The CESE method can be categorized as a cell-centered finite volume method. It aims to solve unsteady flow problems. The core ideas that motivated the development of the CESE method are (1) enforcing flux conservation over a discretized space-time domain, (2) constructing a nondissipative scheme as a baseline to fully control the numerical dissipation, (3) avoiding the Riemann solver and dimensional splitting by using a staggered mesh in space and time while maintaining robust handling of shock waves and discontinuities, (4) using a compact stencil (use immediate neighboring cells and/or points), and (5) using unstructured meshes for ease of dealing complex geometries.

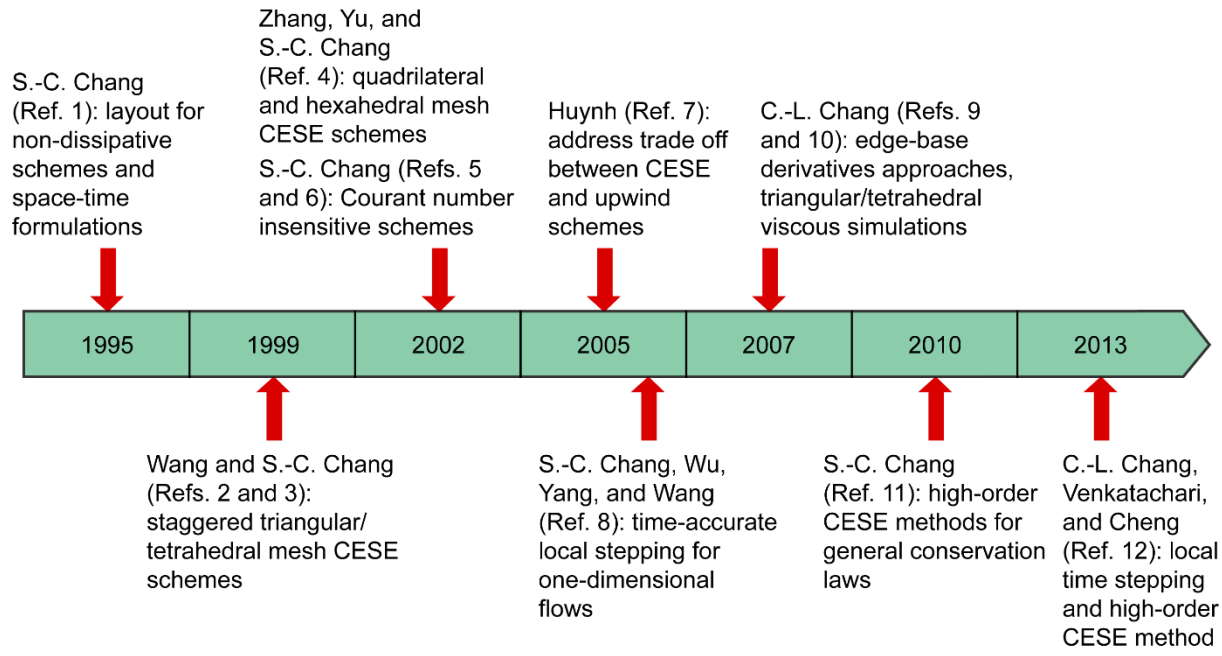

Figure 1.—Timeline of CESE method development.

The CESE method has been used to solve computational aeroacoustic (CAA) benchmark problems involving fan noise and jet noise (Refs. 15 to 20). All problems were successfully solved as blind tests; numerical solutions were compared with analytical solutions and showed good agreement, demonstrating the ability of the CESE method to solve complicated flow physics (e.g., shocks + waves + eddies). In References 21 to 25, the capability of the CESE method for solving engineering problems including high-speed flows with shock waves are demonstrated.

However, some issues remain, such as

(1) The CESE solver becomes very dissipative when the CFL number is small (<<1); here, either a CFL-insensitive scheme might help (Refs. 5 and 6) or local time stepping for a time-accurate solution would be possible way to remedy this (Ref. 8).

(2) A highly stretched viscous mesh near the wall might degrade the accuracy of the gradients of the marching variables. There are a few ways to get better accuracy of the gradients; these can be found in References 7 and 14. Recently, a higher order CESE scheme (fourth-order) has been developed (Refs. 11 to 13), which might enhance accuracy for the viscous flow problems that are dominated by boundaries that are solid walls.

2.0 Discretization

In the following, the numerical scheme is constructed for the 2D and 3D Euler equations using the CESE method. The governing equations are introduced, then the control volume is described in comparison with the traditional methods, and the CESE 2D and 3D Euler solvers are presented.

2.1 The Governing Equations

The 3D Euler equations in conservation form are

$$\frac{\partial u_m}{\partial t}+\frac{\partial e_m}{\partial x}+\frac{\partial f_m}{\partial y}+\frac{\partial g_m}{\partial z}=0, \qquad m=1,2,3,4,5 \tag{1}$$

where u_m are the conservative variables and e_m, f_m, and g_m are the x-, y-, and z-component inviscid fluxes that are defined as follows:

$$u_1=\rho,\ u_2=\rho u,\ u_3=\rho v,\ u_4=\rho w,\ u_5=\rho e_t \tag{2}$$

$$e_1=\rho u,\ e_2=\rho u^2+p,\ e_3=\rho uv,\ e_4=\rho uw,\ e_5=(\rho e_t+p)u \tag{3}$$

$$f_1=\rho v,\ f_2=\rho vu,\ f_3=\rho v^2+p,\ f_4=\rho vw,\ f_5=(\rho e_t+p)v \tag{4}$$

$$g_1=\rho w,\ g_2=\rho wu,\ g_3=\rho wv,\ g_4=\rho w^2+p,\ g_5=(\rho e_t+p)w \tag{5}$$

Here ρ is density, *(u,v,w)* are velocity components, p is pressure, and e_t is the total energy per unit mass.

Its integral form for a finite control volume V in space (x,y,z) is

$$\iiint_V\left(\frac{\partial u_m}{\partial t}+\frac{\partial e_m}{\partial x}+\frac{\partial f_m}{\partial y}+\frac{\partial g_m}{\partial z}\right)\mathrm{d}V=0 \tag{6}$$

Defining $\vec{h}_m=(e_m,f_m,g_m)$ in (x,y,z), Equation (6) then becomes

$$\iiint_V\frac{\partial u_m}{\partial t}\mathrm{d}V+\iiint_V\left(\nabla\cdot\vec{h}_m\right)\mathrm{d}V=0 \tag{7}$$

with $\nabla=\left(\frac{\partial}{\partial x},\frac{\partial}{\partial y},\frac{\partial}{\partial z}\right)$. Using Gauss's theorem, the volume integration in Equation (7) can be converted into surface integration:

$$\iiint_V\frac{\partial u_m}{\partial t}\mathrm{d}V+\oint_{s(V)}\vec{h}_m\cdot\mathrm{d}\vec{s}=0 \tag{8}$$

where *s(V)* is the boundary of the finite volume V.

Equation (8) can be discretized using different traditional numerical methods. The volume integration of the time derivative allows people to use a different discretization approach for the time derivatives, which may be desirable for saving computational time, obtaining higher accuracy for steady-state solutions, or maintaining flux conservation in both space and time for transient problems.

Contrary to the standard approach outlined in Equations (6), (7), and (8), with the CESE method we define $\vec{h}_m=(e_m,f_m,g_m,u_m)$ in space and time (x,y,z,t), and Equation (6) becomes

$$\iiint_V\left(\nabla\cdot\vec{h}_m\right)\mathrm{d}V=0 \tag{9}$$

where $\nabla = \left(\frac{\partial}{\partial x}, \frac{\partial}{\partial y}, \frac{\partial}{\partial z}, \frac{\partial}{\partial t} \right)$ and V is a finite control volume in space and time. Next, using Gauss's theorem and converting the volume integration in Equation (9) into surface integration:

$$\oint_{s(V)} \vec{h}_m \cdot \mathrm{d}\vec{s} = 0 \tag{10}$$

The CESE method is about the discretization of Equation (10). Note that the integral form of the Euler equation in Equation (10) is the original form of conservation laws. Equations (1) and (7) can be derived from Equation (10) only if the flow is continuous. For the time derivative term, CESE does surface integration instead of volume integration, which results in no ambiguity for the discretization of the time derivative term. Also, the scheme is second-order accurate in both space and time. The flux conservation in both space and time is guaranteed.

In the following section, the discretization of Equation (10) will be described using a staggered (CESE method) versus nonstaggered (traditional method) control volume. A 2D unstructured triangular mesh is used as an example to explain how to construct a scheme for Equation (10) based on the CESE method in comparison with traditional methods.

2.2 Control Volume (Traditional Method Versus CESE Method)

Figure 2 shows an unstructured triangular mesh as an example. Consider a triangle, ΔBDF, which has three neighboring triangles. Let points A, C, and E be the centroids of those three neighboring triangles. With the traditional method, each triangle will be the control volume where the flux is assumed to be conserved. The solution point is at the center of each triangle. Then an interface exists between neighboring control volumes. Each interface is associated with multiple solution points. Therefore, the uniqueness and smoothness of the interface flux has to be addressed. Most of the time, the interface flux is computed using the solution point on the upwind side, a mixture of both sides, or an average of both sides, which results in the various classes of upwind and central differencing schemes.

In the CESE method, for the triangle ΔBDF, the control volume is the hexagon ABCDEF formed by connecting the three neighboring centroids to the vertices of the triangle ΔBDF. One of the neighboring triangles of ΔBDF is ΔDIF, and the corresponding control volume is the hexagon FGDHIJ. Note that there is no interface between the control volumes of two neighboring triangles, but the two control volumes overlapped on GDEF. The solution point will be the geometric center of the hexagon, not the geometric center of the triangle. Each triangle is associated with a hexagon and a solution point, which again is the centroid of the hexagon.

The conservation element (CE) is the same as the traditional control volume but in both space and time. The solution element (SE) is the boundary of the CE for each solution point, also in space and time. For an example, the CE for point G is the hexagonal cylinder with the base of the hexagon ABCDEF, and the SE will be the boundary surfaces of the hexagonal cylinder.

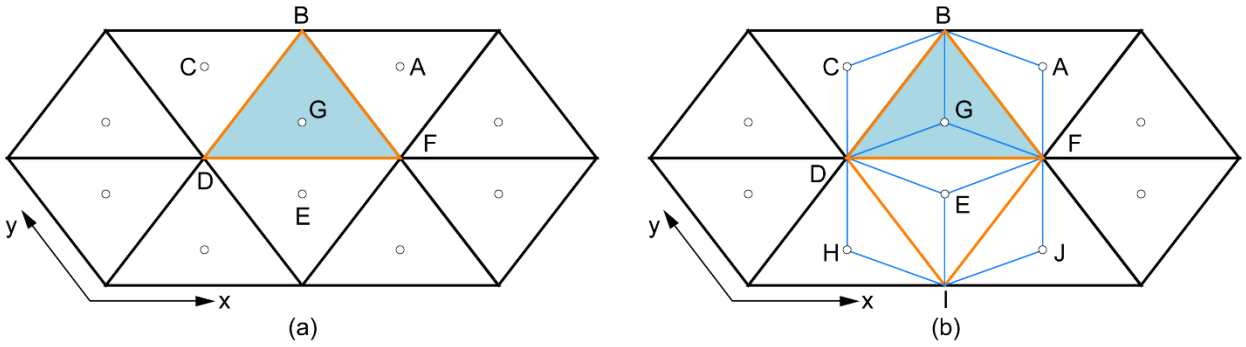

Figure 2.—Control volumes for discretization of Euler equations. (a) Traditional method. (b) Conservation Element and Solution Element (CESE) method.

Within the SE associated with a solution point (j,n), the numerical approximation of $\vec{h}_m = (e_m, f_m, g_m, u_m)$ is denoted as $\vec{h}_m^* = (e_m^*, f_m^*, g_m^*, u_m^*)$ with

$$u_m^*(x,y,z,t;j,n) = (u_m)_j + (u_{mx})_j(x-x_j) + (u_{my})_j(y-y_j) + (u_{mz})_j(z-z_j) + (u_{mt})_j(t-t^n) \tag{11}$$

$$e_m^*(x,y,z,t;j,n) = (e_m)_j + (e_{mx})_j(x-x_j) + (e_{my})_j(y-y_j) + (e_{mz})_j(z-z_j) + (e_{mt})_j(t-t^n) \tag{12}$$

$$f_m^*(x,y,z,t;j,n) = (f_m)_j + (f_{mx})_j(x-x_j) + (f_{my})_j(y-y_j) + (f_{mz})_j(z-z_j) + (f_{mt})_j(t-t^n) \tag{13}$$

$$g_m^*(x,y,z,t;j,n) = (g_m)_j + (g_{mx})_j(x-x_j) + (g_{my})_j(y-y_j) + (g_{mz})_j(z-z_j) + (g_{mt})_j(t-t^n) \tag{14}$$

For the CE at (j,n), Equation (10) becomes

$$\oint_{s(CE)} \vec{h}_m^* \cdot d\vec{s} = 0 \tag{15}$$

Details on solving Equation (15) will be given in Section 2.5, Three-Dimensional Formulation. Here the difference between the traditional and CESE methods is summarized in Table I, using ΔBDF as an example.

TABLE I.— COMPARISON BETWEEN TRADITIONAL (UPWIND) AND CONSERVATION ELEMENT AND SOLUTION ELEMENT (CESE) METHODS
[Points A through G are illustrated in Figure 2.]

Definition	Upwind scheme	CESE scheme	Comments on CESE
Control volume (CV)	ΔBDF (triangle, nonoverlap)	ABCDEF (hexagon, partially overlap)	Inflated CV, but the same stencil
Boundary of CV	BD, DF, and FB (3)	AB, BC, CD, DE, EF, and FA (6)	Doubled number of boundaries
Number of interfaces between CVs of two neighboring triangles	Three	Zero (no interface)	No need to consider interface fluxes
Number of solution points each boundary of CV is associated with	Two	One	Solution point is on the boundary
How flux at center of boundary is computed	Taylor series expansion from left and right and then upwind flux	Taylor series expansion from the solution point	Uniquely defined
Example	For BD, use solution at either C or G or both based on upwind	For BC (and CD), use the solution at C	Sum fluxes through all boundaries to update solution at G

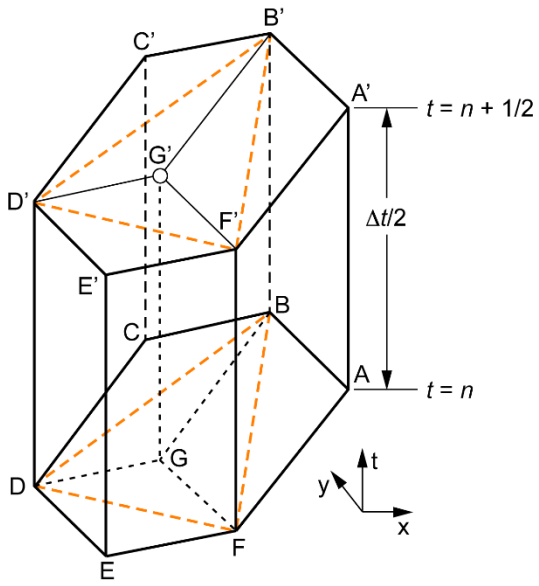

Figure 3.—Conservation element (CE) in (x, y, *t*) for two-dimensional mesh.

2.3 Time-Marching for the Primary Unknowns $(u_m)_j^{n+1/2}$ With CESE Method

Figure 3 shows the control volume associated with the triangle ΔBDF in space and time (x,y,t). Given the solution at points A, C, and E at time level *n,* the solution at point G' at $t = n+1/2$ is updated. Each solution point at $t = n$ is associated with two surfaces of the control volume along the time direction and one surface at a constant time level. The flux is computed at the geometric center of each surface from the solution point based on a Taylor series expansion. For the surface on the top (time level $n+1/2$), the flux is simply the solution at the geometric center of the hexagon multiplied by the surface area. Some details are given as follows.

(1) Considering the neighboring point A(j_1,n)

Compute $\vec{h}_m^* = (e_m^*, f_m^*, u_m^*)$ at the centroid of surface A'B'BA (A'F'FA) using the Taylor series expansion from the solution point A as shown in Equations (11) to (14), then multiply the surface area, $\Delta s_{j1,1}$ ($\Delta s_{j1,2}$), and its normal vector in the form of $\vec{n} = (n_x, n_y, 0)$. For the surface of ABGF, where time is constant, again compute $\vec{h}_m^* = (e_m^*, f_m^*, u_m^*)$ at the centroid of the surface ABGF that has the normal vector in the form of $\vec{n} = (0, 0, 1)$ and an area of $\Delta s_{j1,0}$, and then we have the flux

$$R_{j1}^n = \sum_{k=1}^{2} (e_m^* n_x + f_m^* n_y)_{j1,k} \times \Delta s_{j1,k} + (u_m^*)_{j1,0} \times \Delta s_{j1,0} \tag{16}$$

(2) Repeat the same procedure for the second neighboring solution point C(j_2,n) to get the flux (R_{j2}^n) through the surface of B'C'CB, C'D'DC, and CDGB.

(3) Repeat the same procedure for the third neighboring point E(j_3,n) to get the flux (R_{j3}^n) through E'D'DE, E'F'FE, and EFGD.

(4) At $t = n+1/2$, the surface A'B'C'D'E'F' whose area is denoted as Δs_j, the flux is simply $\Delta s_j (u_m)_j^{n+1/2}$ because the solution point is located at the geometric center of the hexagon ABCDEFG.

(5) Summing all fluxes through the CE for solution point G'(j,n+1/2) based on Equation (15) will give

$$\Delta s_j (u_m)_j^{n+1/2} = -(R_{j1}^n + R_{j2}^n + R_{j3}^n) \tag{17}$$

which gives the explicit time-marching scheme to update $(u_m)_j^{n+1/2}$. The stability condition of the scheme is CFL < 1.

2.4 Update the Gradients

A weighted-average limiter based on the gradient amplitude is used to compute u_{mx} and u_{my} at G using the three neighboring solution points (A, C, and E) (Fig. 4).

Three sets of gradients, such as $\left(u_{mx}^{(l)}, u_{my}^{(l)}\right)$, where l = 1,2,3, can be computed using the three planes GAC, GCE, and GEA using a finite-difference approach. Define $q_{m,l} = \sqrt{(u_{mx}^{(l)})^2 + (u_{my}^{(l)})^2}$, and $w_{m,1} = (q_{m,2} q_{m,3})^{\alpha}, w_{m,2} = (q_{m,1} q_{m,3})^{\alpha}, w_{m,3} = (q_{m,1} q_{m,2})^{\alpha}$, where $\alpha = 0,1,2$. The weighted-average limiter is

$$u_{mx} = \frac{w_{m,1} u_{mx}^{(1)} + w_{m,2} u_{mx}^{(2)} + w_{m,3} u_{mx}^{(3)}}{w_{m,1} + w_{m,2} + w_{m,3}}, u_{my} = \frac{w_{m,1} u_{my}^{(1)} + w_{m,2} u_{my}^{(2)} + w_{m,3} u_{my}^{(3)}}{w_{m,1} + w_{m,2} + w_{m,3}} \tag{18}$$

Equation (18) is the original way of computing the gradients proposed by S.C. Chang (Ref. 2). In Reference 6, S.C. Chang describes a modified version of Equation (18) to provide better accuracy of gradients of the time-marching variables.

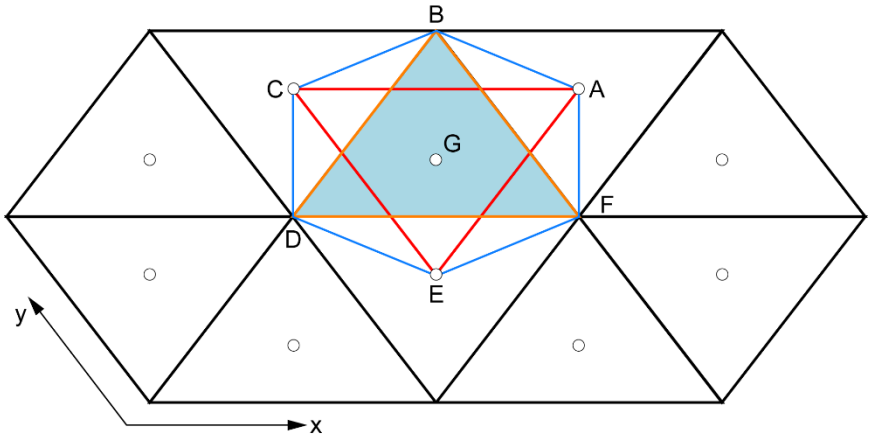

Figure 4.—Stencil used to compute derivatives.

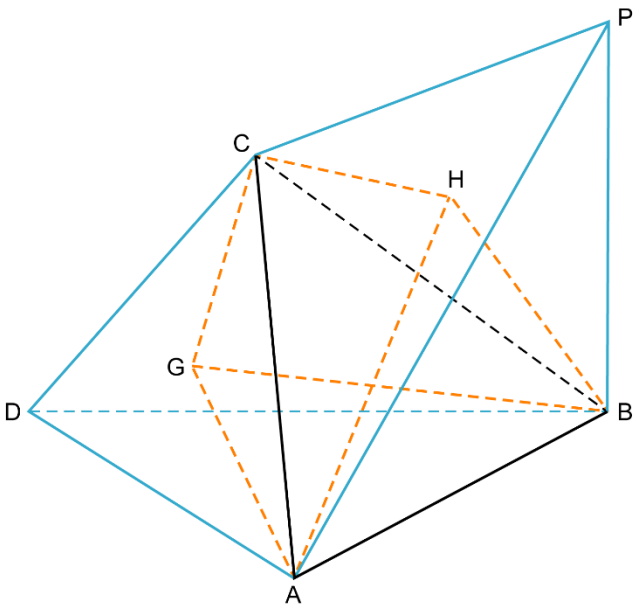

Figure 5.—Subconservation element related to three-dimensional tetrahedral mesh.

2.5 Three-Dimensional Formulation

Consider a tetrahedron ABCD in Figure 5, in which one of its four neighboring tetrahedrons ABCP is also plotted. The tetrahedron shares the face ABC. Points G and H are the centroids of ABCD and ABCP, respectively. The polyhedron GABCH is the subconservation element (sub-CE) associated with solution point G.

Similarly, three additional sub-CEs associated with point G can be constructed by considering in turn the three tetrahedrons that share one of its other three surfaces with ABCD. The summation of the four sub-CEs will be the CE, the control volume where flux is assumed to be conserved. It includes the tetrahedron itself (ABCD) and one-fourth of each of its neighboring tetrahedrons. The solution point is located at the geometric center of the CE, which is not necessarily at the center of the tetrahedron.

The control volume in space and time (x,y,z,t) cannot be plotted. The solution at point G'(j,n+1/2) is updated using four neighboring solution points at time level n. Each solution point at $t = n$ is associated with three volumes of the control volume along the time direction and one volume at constant time. The flux is computed at the geometric center of each volume from the solution point based on a Taylor series expansion. At the volume on the top (time level n+1/2), the flux is simply the solution at the geometric center of the CE multiplied by its volume. The fluxes are then summed over the control volume based on Equation (15). Some details are given as follows.

1. Considering the neighboring point H(j_1,n)

   Compute $\vec{h}_m^* = (e_m^*, f_m^*, g_m^*, u_m^*)$ at the centroid of volume HABH'A'B' (HACH'A'C' and HBCH'B'C') using a Taylor series expansion from the solution point H, then multiply the volume $\Delta v_{j1,k}$, where k = 1,2,3 and the normal vector of the surface HAB (HAC, HCB) that is in the form of $\vec{n} = (n_x, n_y, n_z, 0)$. (H',A',B',C' is the extrusion of the point H,A,B,C in the time direction, not plotted in the figure.) For the volume GABCH, where time is constant ($t = n$), again compute

$\vec{h}_m^* = (e_m^*, f_m^*, g_m^*, u_m^*)$ at the centroid of the volume GABCH that has the normal vector in the form of $\vec{n} = (0,0,0,1)$ and volume of $\Delta v_{j1,0}$. We have the flux

$$R_{j1}^n = \sum_{k=1}^{3} (e_m^* n_x + f_m^* n_y + g_m^* n_z)_{j1,k} \times \Delta v_{j1,k} + (u_m^*)_{j1,0} \times \Delta v_{j1,0} \tag{19}$$

2. Repeat the same procedure for the rest of the volumes associated with the other three neighboring solution points to get the fluxes $R_{j2}^n, R_{j3}^n, \text{and } R_{j4}^n$.

3. At $t = n + 1/2$, the volume of the CE is Δv_j, and the flux is simply $(u_m)_j^{n+1/2} \cdot \Delta v_j$ because the solution point is located at the geometric center of the CE.

By summing all fluxes through the CE for solution point G'(*j, n+1/2*), Equation (15) yields

$$\Delta v_j (u_m)_j^{n+1/2} = -(R_{j1}^n + R_{j2}^n + R_{j3}^n + R_{j4}^n) \tag{20}$$

which results in the explicit time marching scheme for $(u_m)_j^{n+1/2}$. The gradients can be easily extended to 3D formulation based on Equation (18) and will not be repeated here.

The location where the flux is computed at the boundary of the CE is summarized in Table II to give readers a better idea how it is defined.

TABLE II.—LOCATION OF THE FLUX IS COMPUTED IN ONE, TWO, AND THREE DIMENSIONS

Dimension	Boundary of conservation element (CE) along the time direction	Boundary of CE at $t = n$
3D	Three surfaces, geometry center of each surface, time is at $t = t^n + \mathrm{d}t/4$	One volume, center of the volume, $t = t^n$
2D	Two lines, geometry center of each line, time is at $t = t^n + \mathrm{d}t/4$	One surface, center of the surface, $t = t^n$
1D	One point, at that point, time is at $t = t^n + \mathrm{d}t/4$	One line, center of the line, $t = t^n$

2.6 CESE Nondissipative Scheme

The schemes in Equation (17) for 2D and Equation (20) for 3D are used in most computations of Euler flow. With the weighted-average limiter, the numerical dissipation is adjusted from the nondissipative scheme with added numerical dissipation as needed. The nondissipative scheme is the foundation of the CESE scheme and guides the CESE scheme construction under a set of rigorous rules (Ref. 1). When solving real problems, how much dissipation is needed depends on the physics of the problem. In general, numerical dissipation has to be less than the physical viscosity in order to obtain the correct physical solution. Sometimes the physical viscosity is extremely small, and then it requires the scheme to be highly accurate yet stable.

For the 2D case described in Section 2.2, Control Volume (Traditional Method Versus CESE Method), the conservation element in space is defined as the hexagon ABCDEF. It can be seen that the hexagon is formed by three quadrilaterals, ABGF, BCDG, and DGEF, that can be defined as three sub-CEs. Assuming Equation (15) is true for the three sub-CEs, there will be three equations for three unknowns $(u_m)_j^{n+1/2}, (u_{mx})_j^{n+1/2}, \text{and} (u_{my})_j^{n+1/2}$ for each *m*. For the 3D case, each conservation element has four sub-CEs that yield four equations for four unknowns $(u_m)_j^{n+1/2}, (u_{mx})_j^{n+1/2}, (u_{my})_j^{n+1/2}, \text{and} (u_{mz})_j^{n+1/2}$ for each *m*. The marching variable $(u_m)_j^{n+1/2}$ and its spatial derivatives are solved using the conservation laws for the nondissipative CESE scheme.

2.7 CESE Fourth-Order Scheme Compared to Traditional Methods

The fourth-order CESE Euler solver has been developed recently. Validation and assessment is under way (Refs. 12 and 13). The stencil and control volume used in the fourth-order scheme is the same as that used in the second-order scheme. The time-marching scheme is the same as that of the second-order scheme, but it is used twice. First, the differentialized governing equation for the higher order derivatives (u_{xx} and u_{xxx}) is solved; then the original governing equation for u and u_x is solved. Higher order Taylor series expansion is used to compute the flux on the boundary of control volume. The stability condition is CFL < 1, the same as for the second-order scheme. The shock-capturing limiter is the same as that for the second-order scheme. Upwinding is not needed since the flux is uniquely computed at the interface. The traditional high-order finite-volume methods use a high-order polynomial to represent the solution inside each cell. They (1) divide each cell into the subgrid based on the order of accuracy, (2) decide the polynomial coefficients using the subgrid solution, and (3) reconstruct the flux on the interface of the control volume. Note this has to be carefully handled since the accuracy of the scheme is highly dependent on this. The higher the order of accuracy, the more restricted the stability conditions become; that is, the smaller the time step size will be.

3.0 Discussion

The CESE scheme has some concepts that are similar to those that were previously described in the literature.

Space-time formulation was mentioned in Roe's paper in 1983 (Ref. 26), but the importance of the space-time formulation for the scheme's accuracy was not discussed. CESE emphasizes space-time flux conservation and applies it to the discretization scheme. Given that flux conservation is applied in space and time, there is no ambiguity on how to discretize the time derivative terms with the CESE method.

A staggered mesh was used by Nessyahu and Tadmor (N-T) on a 2D quadrilateral mesh in 1990 (Ref. 27); but it was not extended to a triangular mesh for 2D or any 3D formulation. The CESE method is consistent in its formulation for one, two (triangle), and three (tetrahedron) dimensions. Also, the N-T scheme does not have a nondissipative scheme. The CESE nondissipative scheme is the core of the scheme development.

The weighted-average limiter was proposed by van Albada in 1982 (Ref. 28), but it is for a 1D formula; the triangular mesh version of the corresponding limit was not developed. The CESE method has a coherent formulation of the weighted-average limiter from one, two, and three dimensions, which works robustly for capturing discontinuities, such as shock waves and contact surfaces.

Staggered versus nonstaggered control volumes is the major difference between the CESE and traditional methods. Although a staggered control volume avoids the interface so there is no need of upwinding for the flux at the interface, its effect on the overall performance of the scheme compared with that of a nonstaggered control volume needs to be further evaluated using real engineering problems; that is, 3D unsteady viscous turbulent flows. The performance of the scheme includes the cost (computation time), accuracy, and robustness. These efforts are underway.

4.0 Concluding Remarks

The Conservation Element and Solution Element (CESE) method for solving conservation laws has been described and compared with other traditional methods. The numerical schemes for both two- and three-dimensional Euler equations were illustrated based on the CESE method. The major differences and similarities between the CESE method and other traditional methods have been highlighted and addressed from different perspectives.

References

1. Chang, Sin-Chung: The Method of Space-Time Conservation Element and Solution Element—A New Approach for Solving the Navier-Stokes and Euler Equations. J. Comput. Phys., vol. 119, no. 2, 1995, pp. 295–324.
2. Chang, S.-C.; and Wang, X.-Y.: A 2D Non-Splitting Unstructured Triangular Mesh Euler Solver Based on the Space-Time Conservation Element and Solution Element Method. Computational Fluid Dynamics Journal, vol. 8, no. 2, 1999, p. 309.
3. Wang, Xiao-Yen; and Chang, Sin-Chung: A 3D Non-Splitting Structured/Unstructured Euler Solver Based on the Space-Time Conservation Element and Solution Element Method. AIAA–99–3278, 1999.
4. Zhang, Zeng-Chan; Yu, S.T. John; and Chang, Sin-Chung: A Space-Time Conservation Element and Solution Element Method for Solving the Two- and Three-Dimensional Unsteady Euler Equations Using Quadrilateral and Hexahedral Meshes. J. Comput. Phys., vol. 175, 2002, pp. 168–199.
5. Chang, Sin-Chung: Courant Number Insensitive CE/SE Schemes. AIAA 2002–3890, 2002.
6. Chang, S.C.; and Wang, X.Y.: Multi-dimensional Courant Number Insensitive CE/SE Euler Solvers for Applications Involving Highly Nonuniform Meshes. AIAA 2003–5285, 2003.
7. Huynh, H.T.: Analysis and Improvement of Upwind and Centered Schemes on Quadrilateral and Triangular Meshes. AIAA 2003–3541, 2003.
8. Chang, Sin-Chung, et al.: Local Time-Stepping Procedures for the Space-Time Conservation Element and Solution Element Method. International J. Comput. Fluid Dynamics, vol. 19, no. 5, 2005, pp. 359–380.
9. Chang, Chau-Lyan: Time-Accurate Unstructured-Mesh Navier-Stokes Computations With the Space-Time CESE Method. AIAA 2006–4780, 2006.
10. Chang, Chau-Lyan: Three-Dimensional Navier-Stokes Calculations Using the Modified Space-Time CESE Method. AIAA 2007–5818, 2007.
11. Chang, Sin-Chung: A New Approach for Constructing Highly Stable High Order CESE Schemes. AIAA–2010–543, 2010.
12. Chang, Chau-Lyan; Venkatachari, Balaji; and Cheng, Gary: Time-Accurate Local Time Stepping and High-Order Space-Time CESE Methods for Multi-Dimensional Flows With Unstructured Meshes. AIAA 2013–3069, 2013.
13. Bilyeu, David, et al.: A Two-Dimensional Fourth-Order Unstructured-Meshed Euler Solver Based on the CESE Method. J. Comput. Phys., vol. 257, pt. A, 2014, pp. 981–999.
14. Chang, Sin-Chung; Chang, Chau-Lyan; and Yen, Joseph C.: Recent Developments in the CESE Method for the Solution of the Navier-Stokes Equations Using Unstructured Triangular or Tetrahedral Meshes With High Aspect Ratio. AIAA 2013–3068 (NASA/TM—2013-218061), 2013.
15. Wang, Xiao-Yen; Chow, Chuen-Yen; and Chang, Sin-Chung: Numerical Simulations of Gust Generated Aeroacoustics in a Cascade Using the Space-Time Conservation Element and Solution Element Method. AIAA 98–0178, 1998.
16. Wang, Xiao-Yen; Chang, Sin-Chung; and Jorgenson, Philip C.E.: Prediction of Sound Waves Propagating Through a Nozzle Without/With a Shock Wave Using the Space-Time CE/SE Method. AIAA 2000–0222 (NASA/TM—2000-209937), 2000.
17. Wang, X.Y., et al.: Gust Acoustic Response of a Swept Rectilinear Cascade Using the Space-Time CE/SE Method. NASA/TM—2001-210815 (FEDSM−2001–18134), 2001.
18. Wang, X.Y., et al.: Gust Acoustics Response of a Single Airfoil Using the Space-Time CE/SE Method. AIAA–2002–0801 (NASA/TM—2003-211513), 2002.
19. Loh, Ching Y.; Hultgren, Lennart S.; and Chang, Sin-Chung: Wave Computation in Compressible Flow Using the Space-Time Conservation Element and Solution Element Method. AIAA J., vol. 39, no. 5, 2001, p. 794.
20. Loh, Ching-Y.; and Zaman, K.B.M.Q.: Numerical Investigation of Transonic Resonance With a Convergent-Divergent Nozzle. AIAA J., vol. 40, no. 12, 2002, p. 2393.

21. Chang, Chau-Lyan; Choudhari, Meelan M.; and Li, Fei: Numerical Computations of Hypersonic Boundary-Layer Over Surface Irregularities. AIAA 2010–1572, 2010.
22. Chang, Chau-L., et al.: Effects of Cavities and Protuberances on Transition Over Hypersonic Vehicles. AIAA 2011–3245, 2011.
23. Wang, Bao; He, Hao; and Yu, S.-T. John: Direct Calculation of Wave Implosion for Detonation Initiation. AIAA J., vol. 43, no. 10, 2005, pp. 2157–2169.
24. Tseng, T.I.; and Yang, R.J.: Simulation of the Mach Reflection in Supersonic Flows by the CE/SE Method. Shock Waves, vol. 14, no. 4, 2005, pp. 307−311.
25. Liu, Kaixin, et al.: A Review on the CE/SE Method. Adv. in Mech., vol. 41, no. 4, 2011, pp. 447−461.
26. Roe, P.L.: An Introduction to Numerical Methods Suitable for the Euler Equations. VKI for Fluid Dynamics Lecture Series 1983−01, von Karman Institute for Fluid Dynamics, Belgium, 1983.
27. Nessyahu, Haim; and Tadmor, Eitan: Non-oscillatory Central Differencing for Hypersonic Conservation Laws. J. Comput. Phys., vol. 87, no. 2, 1990, pp. 408−463.
28. van Albada, G.D.; van Leer, B.; and Roberts, W.W., Jr.: A Comparative Study of Computational Methods in Cosmic Gas Dynamics. Astron. Astrophys., vol. 108, no. 1, 1982, pp. 76−84.